

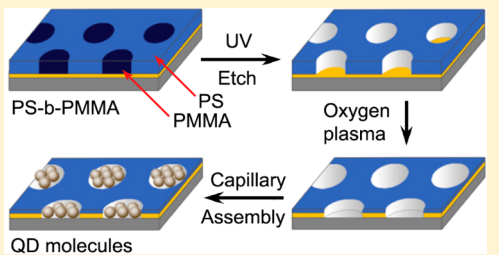
Template-Assembly of Quantum Dot Molecules

Kin Wai Lei, Tyler West, and X.-Y. Zhu*

Texas Materials Institute and Department of Chemistry & Biochemistry, University of Texas, Austin, Texas 78712, United States

 Supporting Information

ABSTRACT: Semiconductor quantum dots (QDs) have been called artificial atoms because of their discrete electronic structures. Assembling them into artificial molecules may greatly expand our capability in controlling physical properties on the nanoscale. Here we show the successful assembly and size control of colloidal PbSe QD clusters into large-scale templates defined by block-copolymer patterns. Following the exchange of capping molecules, the QD clusters behave as artificial molecules due to enhanced and local electronic interactions.



1. INTRODUCTION

The magic of chemistry lies in the myriad possibility of achieving new and controlled physical properties from the assembly of a relatively small number of building blocks, i.e., atoms. This fundamental principle is now being explored in nanomaterials research. Semiconductor nanocrystals or quantum dots (QDs) have been referred to as artificial atoms because of their discrete energy levels near the band edges. An exciting prospect is to assemble them into artificial molecules¹ to achieve new and controlled electronic structures and charge/energy transfer dynamics for a wide range of applications, e.g., electronics and optoelectronics. Alivisatos and co-workers^{2,3} and Buck et al.⁴ have attempted the direct synthesis of QD molecules based on bonding of QDs with inorganic interconnections. A more general approach is to assemble artificial molecules from colloidal QDs. A number of studies reported the assembly of colloidal QDs into close packed QD films or superlattices.^{5–7} To increase inter-QD electronic interaction, one can remove or replace the long and insulating capping molecules by shorter or conjugated ones,^{8–10} but this approach leads to QD solids or clusters with random size distributions. For clusters of colloidal QDs to behave as artificial molecules, there must be not only inter-QD electronic interaction but also well-defined and controlled size distribution.

Here we explore the use of geometric templates and capillary force assembly to achieve large-scale synthesis of colloidal QD molecules. This assembly strategy is based on the presence of capillary force acting on nanoparticles when the solvent front of the colloidal solution is dragged across a surface with defined topographic features to provide geometrical confinement.¹¹ Capillary force assembly has been used to assemble polystyrene spheres, gold nanoparticles, and gold nanorods onto templates with array of trenches and holes,^{12–15} but the sizes of particles demonstrated so far have been larger than the sizes of semiconductor QDs (≤ 10 nm) and forming ordered assemblies of sub-10 nm particles has been shown to be difficult.¹⁶ To overcome this difficulty and achieve large-scale assembly of

artificial molecules from QDs with diameter < 10 nm, we use block-copolymer templates and control the surface topographical features (heights) to the scale of the diameter of QDs. We find the latter to be essential to the successfully assembly of sub-10 nm QDs.

2. EXPERIMENTAL SECTION

Synthesis of PbSe Capped with Oleate. The protocol used to synthesize the PbSe quantum dots with oleate (OA) capping ligands is detailed elsewhere.²² All chemicals and solvents were used as purchased without further purification unless otherwise stated. The general synthetic route followed the hot-injection method performed in a standard Schlenk line setup under N₂ flow. Monodispersed QDs with diameter around 5 nm and the first exciton absorption peak at 768.5 ± 1 meV in tetrachloroethylene (TCE) solution were characterized on a Hitachi S5500 (Hitachi High Technologies America, Inc.) scanning electron microscope (SEM) in scanning-transmission electron microscopy (STEM) mode and a Cary 5000 UV–vis-NIR spectrometer (Agilent, CA). Figure 1 shows STEM image and absorption spectrum of PbSe-OA (diameter 5.0 ± 0.3 nm) in TCE.

Fabrication of Polymer Template. All polymer samples were purchased from Polymer Source (Montreal, Canada). Three polymers were used: two poly(styrene-b-methyl methacrylate) (PS-b-PMMA) block-copolymers, with number averaged molecular weight of 68000(PS)/33500(PMMA) and 37500(PS)/18000(PMMA), and a random copolymer, poly(styrene-co-methyl methacrylate) with hydroxyl termination (PS-r-PMMA) and 62 mol % PS content. A 1 wt % solution of PS-r-PMMA in toluene was spin-coated on a clean silicon substrate (500 μ m thick p-type silicon substrate, University Wafer, MA) to obtain neutral surface energy. The PS-r-PMMA

Special Issue: Paul F. Barbara Memorial Issue

Received: September 2, 2012

Revised: October 4, 2012

Published: October 17, 2012

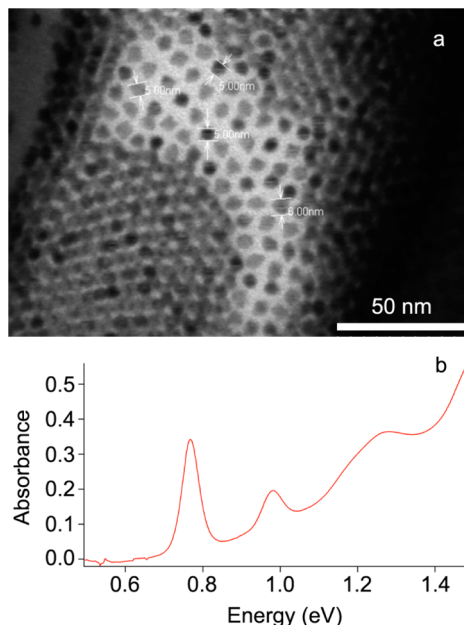


Figure 1. a) STEM image of as-synthesized PbSe (diameter 5.0 ± 0.3 nm) QDs with OA capping molecules. b) Absorption spectra of the OA-capped PbSe-QDs in tetrachloroethylene; 1st exciton = 0.769 ± 0.001 eV, 2nd exciton = 0.979 ± 0.001 eV.

film was thermally annealed in a vacuum oven at 180°C for 72 h and then rinsed with toluene. For the block-copolymer coating, a 1 wt % solution of PS-*b*-PMMA in toluene was spin-coated on the PS-*r*-PMMA layer and thermally annealed in a vacuum oven at 180°C for 24 h. The morphology of annealed film was studied by atomic force microscope (AFM) in tapping mode with a MFP-3D standalone AFM from Asylum Research (Santa Barbara, CA). The AFM tip used was purchased from AppNano (Santa Clara, CA) with resonance frequency between 47 and 76 kHz. After thermal annealing, the PS-*b*-PMMA sample was exposed to 254 nm UV light from a Spectroline (Westbury, NY) UV lamp for 9 h to cross-link the styrene within the PS block and to degrade the PMMA block. The sample was rinsed with glacial acetic acid and 18 MΩ ultrapure water to remove the PMMA domains, leaving the PS matrix on the substrate. To achieve a PS film thickness suitable for the assembly of QDs into small clusters, the acid etched film was etched by O₂ plasma in an Oxford Instruments Plasma Lab 80+ system (Oxford Instruments, UK) at 10 W power to remove part of the PS matrix and the PS-*r*-PMMA layer.

Assembly of QD Clusters and Ligand Exchanges. We assembled the PbSe QDs inside a glovebox by dipping the polymer template into a 10 mg/mL hexane solution of PbSe QDs with a mechanical dip-coater and withdrawing at a speed of 1 mm/s. The as-synthesized PbSe QDs have oleate as their capping ligands. Chemical treatment with 1,2-ethanedithiol (95%, Acros Organics) was performed by dipping the polymer template with assembled QD clusters in a 1 M solution of 1,2-ethanedithiol in acetonitrile.²⁶ The chemicals were used as received without further purification. The polymer template was then dipped in pure acetonitrile for 1 min to wash away residual ligand molecules.

Absorption Spectroscopy. We obtained the absorption spectra of assembled PbSe QDs clusters capped with OA or EDT using attenuated total reflectance Fourier transform infrared (ATR-FTIR) spectroscopy. Specifically, crystalline

silicon ATR waveguides were cut and polished to the shape of a parallelogram with a 45° bevel on both ends ($32\text{ mm} \times 10\text{ mm} \times 1\text{ mm}$). After template formation and QD assembly, we carried out ATR-FTIR spectroscopy measurements inside a glovebox using a Nicolet 6700 FTIR-NIR spectrometer equipped with a Mercury–Cadmium–Telluride detector.

3. RESULTS AND DISCUSSIONS

We use PS-*b*-PMMA diblock copolymer thin films as starting points for the templates. The PS and PMMA blocks microphase separate according to their volume ratio.¹⁷ With the volume ratio of $\sim 70\%$ PS used here, the block-copolymer thin film forms hexagonally packed vertical cylinders of PMMA in the PS matrix, with cylinder diameter tunable in the range of tens of nanometers (14–50 nm).^{18,19} Figures 2a and 2b show

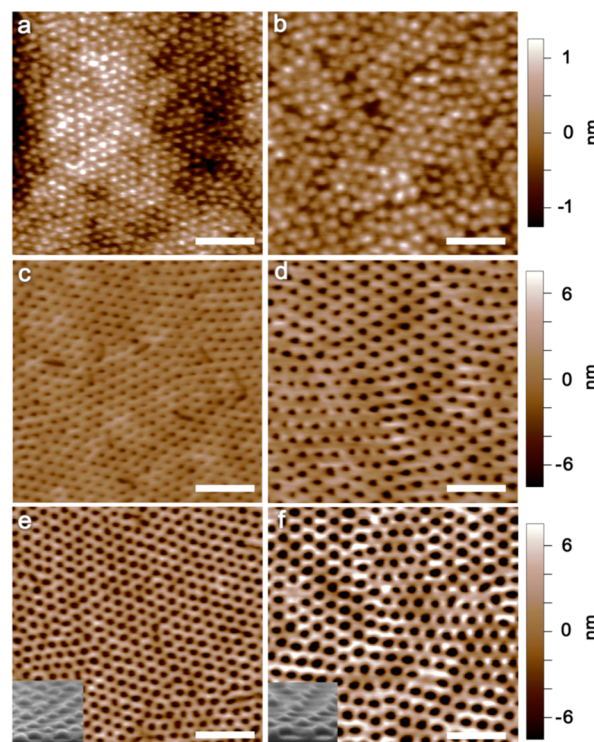


Figure 2. AFM topography images of PS-*b*-PMMA block-co-polymer thin films with molecular weight ratios PS:PMMA = 37.5K:18K (left) and 68K:33.5K (right), respectively. These images were obtained after spin-coating and thermal annealing (a, b), UV cross-linking and chemical etch (c, d), and O₂ plasma etch (e, f). Scale bar = 200 nm. The insets in (e) and (f) show cross sectional SEM images (100 nm \times 100 nm) of the films.

AFM images of the spin-coated and thermally annealed thin films with molecular weight ratios (PS:PMMA) of 37.5K:18K (left) and 68K:33.5K (right), respectively. The images clearly show the hexagonally ordered PMMA cylinders in the PS matrix, with both cylinder diameter and intercylinder distance increasing with molecular weight. After UV irradiation and acetic acid washing, the film form hexagonally packed holes within a PS matrix, as shown by AFM images in Figures 2c and 2d for the two different molecular weights, respectively. We have studied capillary force assembly of QDs into these holes, but find the aspect ratio (depth/diameter) to be too large to allow for the reproducible filling of the holes with defined sizes, in agreement with a similar attempt by Misner et al.²⁰ To

significantly decrease the aspect ratio, we use reactive oxygen ion etch to decrease the thickness of the polymer thin film. The etching step also widens the holes. We find this last step to be most critical as the smallest aspect ratio (height of PS matrix ~ 10 nm) before the disruption of hexagonally ordered array structure gives the best results for capillary force assembly of QD molecules. Figures 2e and 2f show AFM images of the final templates after reactive oxygen ion etch of the surfaces shown in Figures 2c and 2d, respectively. The dimensions (hole diameter, interhole distance, depth) of the final templates are approximately = (23 nm, 37 nm, 12 nm) and (35 nm, 49 nm, 10 nm), for the two polymers, respectively. The insets in Figure 2e and 2f show cross sectional views of the same samples in SEM.

We use capillary force assembly to deposit two different sizes of PbSe QDs capped with oleate into the holes of the polymer films. They are identified as QD^A and QD^B with diameter of 5.0 ± 0.3 nm and 4.5 ± 0.3 nm respectively in this study. Deposition was carried out with a QD concentration of ~ 10 mg/mL in hexane with a mechanical dip-coater at a withdrawing speed of 1 mm/s. We find this condition to be near optimal in filling all the holes, with a narrow distribution in the number of QDs per hole, as shown by histograms of the two surfaces in Figures 3a and 3b for QD^A . The average

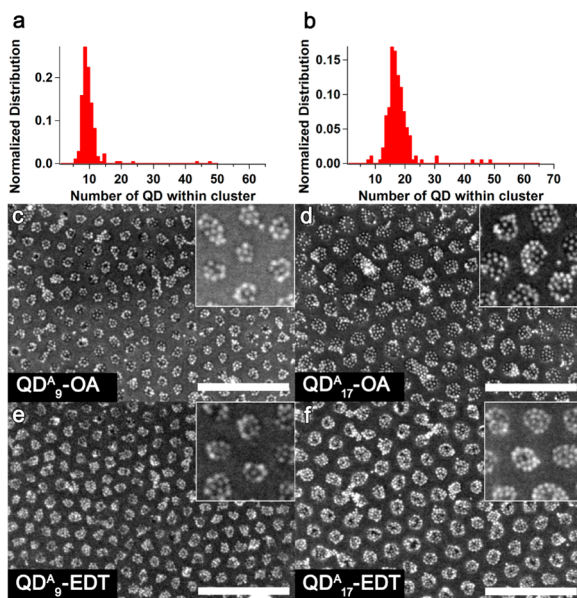


Figure 3. (a,b) Histograms of the number of QDs within each cluster obtained from SEM images of QD^A assemblies on block-copolymer templates before (c,d) or after ligand exchange reaction (OA to DT). Images and data on left (a, c, e) are for QD assemblies on block-copolymer nanopatterns with molecular weight ratio of PS:PMMA = 37.5K:18K and those on the right (b, d, f) with PS:PMMA = 68K:33.5K. Insets in (c, d) show magnified views of the same images. All scale bars = 200 nm.

number of QD^A in each cluster is 9 ± 2 and 17 ± 3 on the two surfaces, with all holes in the templates filled. The corresponding SEM images of QD clusters on the two surfaces are shown in Figure 3c and 3d, for block-copolymer nanopatterns obtained from molecular weight ratios of PS:PMMA = 37.5K:18K and 68K:33.5K, respectively. Each cluster is two-dimensional (2D), with the local arrangement of QDs in each domain near close-packing, but not highly ordered, as shown more clearly by magnified images in Figures

3c and 3d. The hexagonally packed QD clusters extend over macroscopic length scales defined by the polymer coating. Similar deposition condition was used to achieve QD^B clusters using PS:PMMA = 37.5K:18K and 68K:33.5K, with an averaged cluster size of 13 ± 2 and 19 ± 3 , respectively, in accordance with the smaller diameter of QD^B (see the Supporting Information for details).

The results presented above are in stark contrast to previous attempts in assembling QDs into nanohole arrays formed from similar block-copolymer templates. Using the UV etched PS-b-PMMA template, Misner et al. showed that, while some QDs were deposited into the holes, the process was quite random, with a large percentage of holes unfilled and a broad distribution of QDs within the holes.²⁰ We have investigated the correlation between the topographical features and the results of capillary force assembly for templates with different extends (time) of reactive oxygen ion etch. We find that complete filling of all the holes with few QDs on the matrix only occurs when the depth of the holes is of the order of the QDs and the relative surface area of the matrix to that of the holes is small. When the template is etched for too long, the boundaries that form the hexagonal holes in the PS matrix start to break down, leading to the formation of continuous islands of QDs. We find that a sufficiently high concentration of QDs (10 mg/mL) is also necessary for complete hole-filling. When more dilute solutions are used on the same template, the holes are only partially filled. Details on these control experiments can be found in the Supporting Information. Previous studies^{21,22} using X-ray photoelectron spectroscopy and friction force microscopy have shown that exposure to UV and acetic acid leaves behind $-COOH$ functional groups on the PMMA domains. Upon O_2 plasma etching, the PMMA domains are removed while the PS matrix becomes more hydrophilic, likely terminated with $-COOH$ groups^{23,24} that may interact favorably with QDs.²⁵ Although the O_2 plasma treated block-copolymer template shows no contrast in terms of hydrophilicity, we find little adsorption of the QDs on the PS matrix but almost exclusive adsorption into the nanowells. This finding highlights the critical role of aspect ratio in localizing the QD within the nanowells of the template.

Having established the large-scale assembly of QDs, we now turn to their properties. For clusters of QDs to behave like artificial molecules, there needs to be inter-QD electronic interaction. The as-synthesized PbSe QDs are capped with oleic acid molecules that prevent inter-QD electronic interactions. Enhanced electronic coupling between QDs are expected when the long and insulating OA molecules are replaced with much shorter ones, such as 1,2-ethanedithiol (EDT) used in this experiment. Indeed, such a ligand replacement process is known to result in much increased electric conductivity in thin films of PbSe QD solids, as well as significant red-shift in the first exciton peak.^{9,10} Figures 3e and 3f show SEM images of the QD assemblies after the OA ligands have been replaced by EDT molecules in the ligand exchange reaction. The hexagonally arranged QD clusters remain intact, with inter-QD distance within each cluster slightly decreased,²⁶ as also evident in the lower image resolution.

The bottom spectra in Figure 4a show absorption spectra of a monolayer PbSe QD thin film before (blue) and after (red) the ligand exchange reaction (from OA to EDT). The first exciton peak is shifted by -31.6 ± 1 meV (from 764.0 ± 1 meV) following the ligand exchange reaction. While we attributed the red-shift entirely to enhanced inter-QD

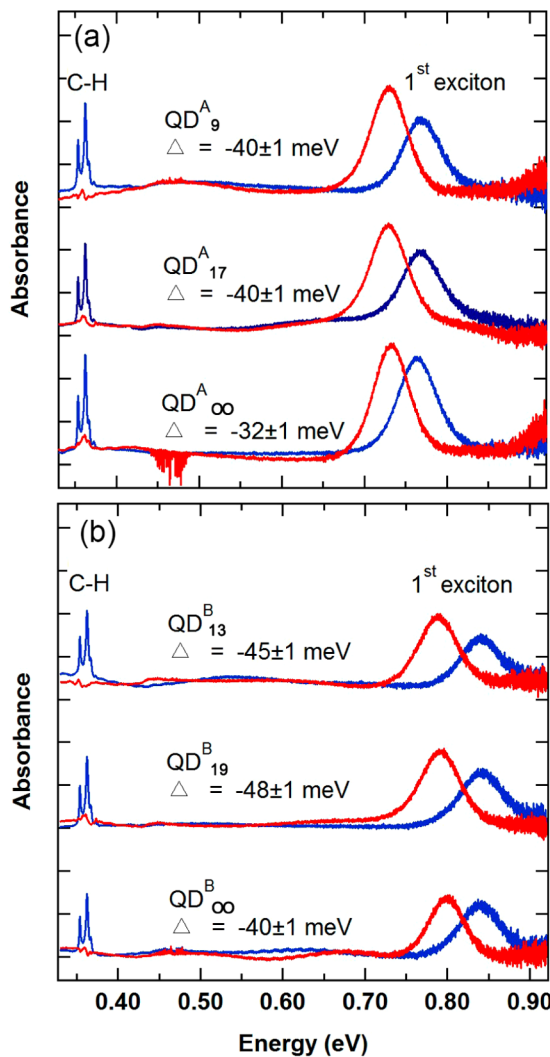


Figure 4. a) Absorption spectra of three PbSe QD^A samples: monolayer film (bottom), QD clusters with average sizes of 17 ± 3 (middle) and 9 ± 2 (top) with OA (blue) and EDT capping (red) molecules. The ligand exchange reaction (from OA to EDT) is characterized by a decrease in the absorbance of the C–H stretch vibrational peak and a red-shift in the first exciton transition. The three sets of spectra are scaled and shifted for clarity. b) The corresponding film and cluster samples for QD^B.

electronic coupling in an earlier study,²⁷ we recently found that, in addition to inter-QD electronic coupling, a major contribution to the red-shift may come from an anomalously large polarization of the dielectric environment surrounding each QD.²⁶ We now compare the excitonic red-shift in monolayer thin film to those in the QD clusters of the two different size distributions (QD^A₉ and QD^A₁₇) on the two block-copolymer templates. For clusters of OA capped QD^As, the first exciton peak is at 769.0 ± 1 meV, independent of cluster size. The slight blue-shift of the first exciton peak in OA capped clusters, as compared to that in the monolayer film, could be explained by the decrease in polarization of the dielectric environment in the former. For both QD^A₉ and QD^A₁₇, exchanging OA with EDT results in red-shifts of 40.0 ± 1 meV. We perform the same ligand exchange from OA to EDT with QD^B to probe how the increased extent of quantum confinement affects the optical red-shift. As shown in Figure 3b, a film of QD^B red-shifted more than a film of QD^A, from 32 ± 1

meV to 40 ± 1 meV. This is in agreement with a previous study²⁶ that smaller QDs give a larger red shift. The same trend of larger red shift with clusters comparing to films is also observed with QD^B₁₃ and QD^B₁₉. Within experiment uncertainty, there is not a significant difference in the red shift between the two cluster sizes for QD^A ($n = 9 \pm 2$ and 17 ± 3) and QD^B ($n = 13 \pm 2$ and 19 ± 3). However, comparison with the two different sizes of QDs confirms that there is a significant enhancement in red shift for clusters of smaller QDs. Note that replacement of OA ligands by EDT also leads consistently to a slight decrease in the width of the first exciton absorption peak, from 32 ± 1 meV to 30 ± 1 meV. This decrease in peak width is not understood and deserves further investigation.

To investigate the dependence of this excitonic red shift on the coupling between neighboring QDs, we performed a series of ligand exchange to QD^A and QD^B films and clusters as a function of inter-QD spacing. In addition to EDT, we also use 1,4-butanedithiol (BDT) and 1,8-octanedithiol (ODT) to replace the oleic acid capping ligands. Using capping molecules with different lengths allows us to control the inter-QD spacing.²⁶ Figure 5 summarizes the result, with each ligand

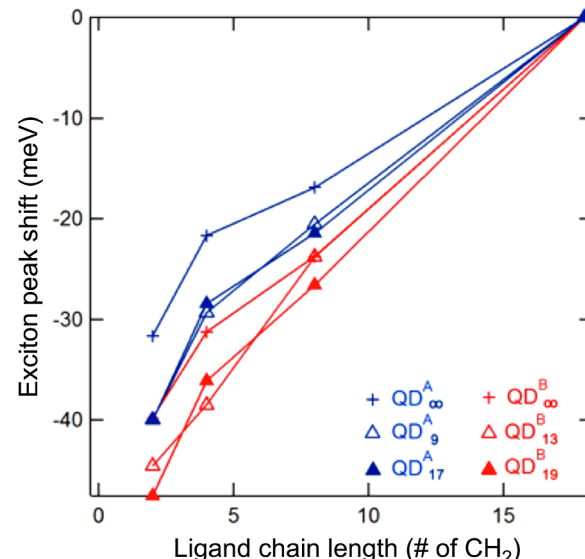


Figure 5. Redshifts in the first exciton transition as a function of the capping ligand length (in number of C atoms in the linking molecules). Blue and red symbols are for PbSe QDs with diameters of 5.0 and 4.5 nm, respectively.

represented by the respective number of carbon atoms between the thiol groups. The red shifts upon ligand exchange are consistently larger for the clusters (QD^A₉, QD^A₁₇, QD^B₁₃, QD^B₁₉) than for the respective 2D films (QD^A_∞ and QD^B_∞). Moreover, a comparison of QD^B with QD^A shows larger redshifts for smaller QDs with stronger quantum confinement.

Although the number of interacting particles in clusters containing a few to a few tens of QDs is expected to be much smaller than that in a monolayer film, the magnitude of the redshift is actually 20% larger than that in the monolayer. The larger red-shift may be attributed to the shorter inter-QD distance following the ligand exchange reaction (from OA to EDT) in a cluster (QD₉ or QD₁₇) than that in a monolayer film, due to the presence of geometric frustration in the later. In a solid thin film consisting of a large number of interacting

QDs, decreasing the inter-QD distance by exchanging long ligand molecules with shorter ones will inevitably build up strain, which counters the chemical bonding force that is bringing the QDs closer. The presence of strain build up is evident by the large number of cracks observed in the QD film following exchange reaction.²⁶ In contrast, this kind of strain is absent for a small QD cluster, thus allowing the inter-QD distance to decrease to the optimal value determined by chemical bonding (between the bifunctional EDT molecule and QD surfaces) and van der Waals interactions.

As we reported before, the excitonic red-shift in PbSe QDs upon ligand exchange can be attributed to a local electronic effect, including enhanced inter-QD electronic interaction and an anomalously large polarization effect,²⁶ which may result from the spatial localization of the exciton wave function to a part of the real nanocrystal, making it very sensitive to changes in local dielectric environment. Such a local electronic/polarization effect argues for the molecular characteristics of the QD clusters. Supporting this argument, we found in previous measurements that there was little excitonic red-shift upon ligand exchange reaction for isolated QDs (i.e., QD₁).²⁷ This result, along with findings on 2D QD clusters presented here, prompted us to ask the following critical question: *what is the size limit of quantum dot molecules where such localized electronic/polarization effects are present*. To answer this question experimentally, we need to reduce the size of QD_n to, e.g., QD₂, QD₃, etc. We have found significant experimental challenges in doing so because of the limitations of the block-copolymer approach in generating high quality patterns of much smaller cylinder sizes than those presented in Figure 2. In addition, capillary force assembly becomes increasingly difficult as the size of the nanowells decreases.¹⁶ We are currently exploring new experimental approaches in overcoming these technical barriers.

4. CONCLUSIONS

We demonstrate the large-scale 2D assembly of artificial molecules with controlled sizes from 5 nm colloidal PbSe QDs using capillary force assembly in nanoscale templates formed from block-copolymer patterns. We find that a crucial factor in successful assembly is a low aspect ratio (depth to diameter) of the nanoholes on the templates, with the depth comparable to the size of the QDs. The method developed here using capillary force assembly is generally applicable to nanoparticles with different sizes and shapes. Optical absorption spectra of the QD clusters with the short capping molecules reveal enhanced and local inter-QD electronic interaction.

■ ASSOCIATED CONTENT

S Supporting Information

Additional SEM images and absorption spectra from control experiments. This material is available free of charge via the Internet at <http://pubs.acs.org>.

■ AUTHOR INFORMATION

Corresponding Author

*E-mail: xyzhu@columbia.edu.

Notes

The authors declare no competing financial interest.

■ ACKNOWLEDGMENTS

This work was supported by the Welch Foundation, grant F-1726. K.W.L. thanks Dr. Abraham Wolcott for help with QD synthesis and Dr. Raluca Gearba with polymer templates. X.Y.Z. wants to dedicate this work to the memory of Paul Barbara, whose infectious vision, enthusiasm, and creativity attracted the author to Austin in 2009. X.Y.Z. will forever treasure the memory of working alongside Paul Barbara for an insanely creative and intense fourteen months in their lives.

■ REFERENCES

- (1) Choi, C. L.; Alivisatos, A. P. *Annu. Rev. Phys. Chem.* **2010**, *61*, 369–389.
- (2) Manna, L.; Scher, E. C.; Alivisatos, A. P. *J. Am. Chem. Soc.* **2000**, *122*, 12700–12706.
- (3) Milliron, D. J.; et al. *Nature* **2004**, *430*, 190–195.
- (4) Buck, M. R.; Bondi, J. P.; Schaak, R. E. *Nat. Chem.* **2012**, *4*, 37–44.
- (5) Murray, C. B.; Kagan, C. R.; Bawendi, M. G. *Science* **1995**, *270*, 1335–1338.
- (6) Shevchenko, E. V.; Talapin, D. V.; O'Brien, S.; Murray, C. B. *J. Am. Chem. Soc.* **2005**, *127*, 8741–8747.
- (7) Kalsin, A. M.; Fialkowski, M.; Paszewski, M.; Smoukov, S. K.; Bishop, K. J. M.; Grzybowski, B. A. *Science* **2006**, *312*, 420–424.
- (8) Talapin, D. V.; Murray, C. B. *Science* **2005**, *310*, 86–89.
- (9) Luther, J. M.; Law, M.; Song, Q.; Perkin, C. L.; Beard, M. C.; Nozik, A. J. *ACS Nano* **2008**, *2*, 271–280.
- (10) Liu, Y.; Gibbs, M.; Puthuserry, J.; Gaik, S.; Ihly, R.; Hillhouse, H. W.; Law, M. *Nano Lett.* **2010**, *10*, 1960–1969.
- (11) Kraus, T.; Malaquin, L.; Schmid, H.; Riess, W.; Spencer, N. D.; Wolf, H. *Nat. Nanotechnol.* **2007**, *2*, 570–576.
- (12) Yin, Y.; Lu, Y.; Gates, B.; Xia, Y. *J. Am. Chem. Soc.* **2001**, *123*, 8718–8729.
- (13) Malaquin, L.; Kraus, T.; Schmid, H.; Delamarche, E.; Wolf, H. *Langmuir* **2007**, *23*, 11513–11521.
- (14) Gordon, M. J.; Peyrade, D. *Appl. Phys. Lett.* **2006**, *89*, 053112–3.
- (15) Kuemin, C.; Stutz, R.; Spencer, N. D.; Wolf, H. *Langmuir* **2011**, *27*, 6305–6310.
- (16) Cui, Y.; Björk, M. T.; Liddle, J. A.; Sönnichsen, C.; Boussert, B.; Alivisatos, A. P. *Nano Lett.* **2004**, *4*, 1093–1098.
- (17) Mansky, P.; Liu, Y.; Huang, E.; Russell, T. P.; Hawker, C. *Science* **1997**, *275*, 1458–1460.
- (18) Thurn-Albrecht, T.; et al. *Adv. Mater.* **2000**, *12*, 787–791.
- (19) Xu, T.; Kim, H. C.; DeRouchey, J.; Seney, C.; Levesque, C.; Martin, P.; Stafford, C. M.; Russell, T. P. *Polymer* **2001**, *42*, 9091–9095.
- (20) Misner, M. J.; Skaff, H.; Emrick, T.; Russell, T. P. *Adv. Mater.* **2003**, *15*, 221–224.
- (21) Asakura, S.; Hozumi, A.; Fuwa, A. *J. Vac. Sci. Technol. B: Microelectron. Nanometer Struct.-Process., Meas., Phenom.* **2005**, *23*, 1137–1140.
- (22) Clear, S. C.; Nealey, P. F. *J. Colloid Interface Sci.* **1999**, *213*, 238–250.
- (23) Ting, Y.-H.; Park, S. M.; Liu, C.-C.; Liu, X.; Himsel, F. J.; Nealey, P. F. *J. Vac. Sci. Technol. B: Microelectron. Nanometer Struct.-Process., Meas., Phenom.* **2008**, *26*, 1684–1689.
- (24) Lianos, L.; Parrat, D.; Hoc, T. Q.; Duc, T. M. *J. Vac. Sci. Technol., A* **1994**, *12*, 2491–2498.
- (25) Wang, M.; Zhang, M.; Siegers, C.; Scholes, G. D.; Winnik, M. A. *Langmuir* **2009**, *25*, 13703–13711.
- (26) Wolcott, A.; et al. *J. Phys. Chem. Lett.* **2011**, *2*, 795–800.
- (27) Williams, K. J.; et al. *ACS Nano* **2009**, *3*, 1532–1538.